Climate Dynamics (2000) 16:93–105

T. N. Chase · R. A. Pielke Sr. · T. G. F. Kittel
R. R. Nemani · S. W. Running

Simulated impacts of historical land cover changes on global climate in northern winter

Received: 8 September 1998 / Accepted: 31 July 1999

Abstract This ten-year general circulation model experiment compared a simulation where land surface boundary conditions were represented by observed, present day land cover to a simulation where the surface was represented by natural, potential land cover conditions. As a result of these estimated changes in historical land cover, significant temperature and hydrology changes affected tropical land surfaces, where some of the largest historical disruptions in total vegetation biomass have occurred. Also of considerable interest because of their broad scope and magnitude were changes in high-latitude Northern Hemisphere winter climate which resulted from changes in tropical convection, upper-level tropical outflow, and the generation of low-frequency tropical waves which propagated to the extratropics. These effects combined to move the Northern Hemisphere zonally averaged westerly jet to higher latitudes, broaden it, and reduce its maximum intensity. Low-level easterlies were also reduced over much of the tropical Pacific basin while positive anomalies in convective precipitation occurred in the central Pacific. Globally averaged changes were small. Comparisons of recent, observed trends in tropical and Northern Hemisphere, mid-latitude climate with these simulations suggests an interaction between the climatic effects of historical land cover changes and other modes of climate variability.

T. N. Chase (✉) · R. A. Pielke Sr.
Department of Atmospheric Science
Colorado State University,
Ft. Collins, CO 80523, USA
E-mail: chase@deathstar.atmos.colostate.edu

T. G. F. Kittel
Climate and Global Dynamics Division,
National Center for Atmospheric Research,
Boulder, CO 80307, USA

R. R. Nemani · S. W. Running
School of Forestry,
University of Montana,
Missoula, MT 59812, USA

1 Introduction

While some of the earliest studies of the effects of the land use change were of global scope (e.g., Sagan et al. 1979 and others reviewed in Mintz 1984), and some recent studies have examined the effects of extratropical land cover change on regional climate (e.g., Bonan et al. 1992; Copeland 1995; Stohlgren et al. 1998), most recent efforts have been understandably concentrated more on regional effects of tropical deforestation and regional desertification because of the vulnerability of these ecosystems and their importance to human populations (e.g., Xue and Shukla 1993; Xue 1997; Claussen 1998). Little acceptance has been given to the idea, however, that anthropogenic land cover changes of the type already observed can significantly influence global climate. Of the few studies which have commented on this subject, McGuffie et al. (1995) noted weak, remote, high-latitude effects in a complete tropical deforestation simulation (i.e., all tropical rainforests converted to grasslands), while Chase et al. (1996) hypothesized that large, winter hemisphere climate anomalies in a simulation of the effects of realistic global green leaf area change were due to tropical deforestation affecting low-latitude convection and therefore global-scale circulations in the winter hemisphere. Zhang et al. (1997) further explored simulated mid-latitude teleconnections due to complete tropical deforestation with a linear wave model and found that appropriate conditions existed for the propagation of tropical waves into the extratropics in that case. Others have since noted isolated extratropical effects due to simulated tropical vegetation physical or physiological changes (Sud et al. 1996, a complete deforestation scenario; Sellers et al. 1996, a study of the effect of increased atmospheric CO_2 on radiation and plant physiology).

It should be expected that changes in tropical land cover affects higher latitudes, particularly in the winter hemisphere. The three major tropical convective heating centers are associated with tropical land surfaces of

Africa, Amazonia, and the maritime continent of Indonesia, Malaysia, New Guinea and surrounding regions (e.g., Kreuger and Winston 1973; Chen et al. 1988; Berbery and Nogués-Paegle 1993). While the existence of the rain-forest and other moist vegetation types has often been considered to be solely a function of local precipitation, significant precipitation recycling does occur due to the presence of transpiring vegetation (e.g. Lettau et al. 1979; Burde and Zangvil 1996). Removal of that vegetation has major impacts on the momentum and radiant energy absorbed at the surface and its partitioning into latent and sensible forms which affect boundary layer energetics and structure and generally culminate in a reduction of precipitation though this seems to be a function of season and region (e.g., Dickenson and Kennedy 1992; Pielke et al. 1997; Zhang et al. 1997; Nobre et al. 1991; Eltahir 1996; Polcher and Laval 1994; Zheng and Eltahir 1997; Eltahir 1998). As a result of removal of tropical vegetation, regional convection might be expected to be reduced in magnitude on average, and shifted in space as a result of compensating circulations and other localized forcings. Small changes in the magnitude and spatial pattern of tropical convection may then alter the magnitude and pattern of high-level tropical outflow which feeds the higher latitude zonal jet (e.g., Bjerknes 1969; Krishnamurti 1961; Chen et al. 1998; Oort and Yienger 1996). Additionally, these changes may also force anomalous Rossby waves which can propogate to high latitudes in a westerly background flow when not trapped by a critical line (e.g., Wallace and Gutzler 1981; Tiedtke 1984; James 1994; Tribbia 1991; Berbery and Nogués-Paegle 1993) and which tend to organize into a few recognizable teleconnection patterns regardless of the spatial nature of convective anomalies (e.g., Geisler et al. 1985; Hoerling and Ting 1994). These forcings may affect weather and climate regimes at high latitudes and are analogous to the remote effects due to anomalous tropical sea surface temperatures during the opposing phases of the El Nino-Southern Oscillation (ENSO).

Our purpose here, then, is to realistically estimate the extent of human impact on global land cover in order to evaluate the hypothesis that these changes, particularly in the tropics, are already of sufficient magnitude to have affected the global climate state through the mechanisms discussed. Building on the work of Chase et al. (1996), we used an updated estimate of global land-cover change in a global numerical model along with comparisons with comparisons with reported observational data.

2 Description of experiment

We used the standard version of the NCAR CCM3 (Kiehl et al. 1996) coupled with the land surface model (LSM) (Bonan 1996). This version of the CCM3 had prescribed SSTs. The LSM is a GCM-scale parameterization of atmospheric-land surface exchanges and accounts for vegetation properties as functions of one of 24 basic vegetation types. The LSM includes a single-level canopy, lake model, and calculates averaged surface fluxes due to subgrid-scale vegetation types and hydrology. Two phenological properties, leaf and stem area index (LAI and SAI), are interpolated between prescribed monthly values. Albedos are calculated as a function of LAI and SAI among other factors. All other vegetation properties are seasonally constant.

Convective precipitation is represented using the schemes of Zhang and McFarlane (1995) for deep convection and that of Hack (1994) for shallow convection. The combined use of these schemes was, in part, responsible for a reduction of the overactive hydrological cycle seen in an earlier version of the model (CCM2) and a more reasonable depiction of the Northern Hemisphere standing wave climatology (Hack et al. 1998).

The CCM3 model was integrated for 12 annual cycles using a representation of current, observed vegetation cover versus a simulation which had a representation of natural, potential vegetation in equilibrium with current climate (an estimate of vegetation undisturbed by human activity) as the bottom boundary condition. The derivation of these datasets is discussed in Sect. 3. Results from this experiment are given in terms of ten averaged Januaries, the month when the maximum communication between the tropics and the Northern Hemisphere is expected. These followed more than two years of model spin-up.

3 Vegetation datasets

Maps of the current and natural vegetation distributions in regions of anthropogenic disturbance are shown in Fig. 1. These datasets were derived with guidance from global maps of maximum LAI which was retrieved for current vegetation from maximum normalized difference vegetation index (NDVI) satellite products (Nemani et al. 1996) at 1° pixel size. Assuming that vegetation is nearly in equilibrium with climate and soils, using long-term precipitation and temperature data, soils data and employing the close empirical relationships between transpiration and LAI (e.g., Nemani and Running 1989), a distribution of maximum LAI for natural, potential vegetation necessary to close the average water budget at each $1 \times 1°$ grid point on the globe was produced (Nemani et al. 1996).

For use in the CCM3, an updated current vegetation dataset was produced simply by declaring regions where the difference between the current and natural maps of maximum LAI was greater than 1 and which were not already agricultural land in the standard CCM dataset (Matthews 1983; Olson et al. 1983) to be anthropogenically disturbed. These anthropogenically disturbed points were assigned one of three kinds of agricultural land in keeping with the standard LSM vegetation categories (irrigated in regions where LAI increased under current vegetation, dryland crop, and mixed crop-forest where LAI decreased) depending on the magnitude of maximum LAI difference, latitude and vegetation type in the standard CCM dataset (Matthews 1983; Olson et al. 1993). That observed vegetation types, such as mixed crop grasslands or mixed crop- and tropical forest are not among the LSM vegetation categories is a source of inaccuracy in the present simulations but we felt it important to stay within the confines of the standard parameterization for these initial simulations.

Despite considering only relatively highly affected regions (Δ LAI > 1) this current vegetation dataset includes larger estimated areas of agricultural land than the standard CCM land cover data particularly in the southeast Asian peninsula, Indonesia, Malaysia, and surrounding regions. Even though larger areas of land cover change were included than in the standard CCM data, our representation of the extent of human land cover disturbance (approximately 15%) remains conservative. A recent estimate (Vitousek et al. 1997) claims over 40% of the Earth's land surface is currently affected by anthropogenic land cover change.

The natural vegetation cover was created by taking the standard CCM dataset and filling in agricultural areas with an appropriate vegetation type. We did this using our estimated potential maximum LAI with values for specific vegetation types roughly following Neilson and Marks (1994), the latitude, and adjacent vegetation for guidance. Differences in vegetation categories

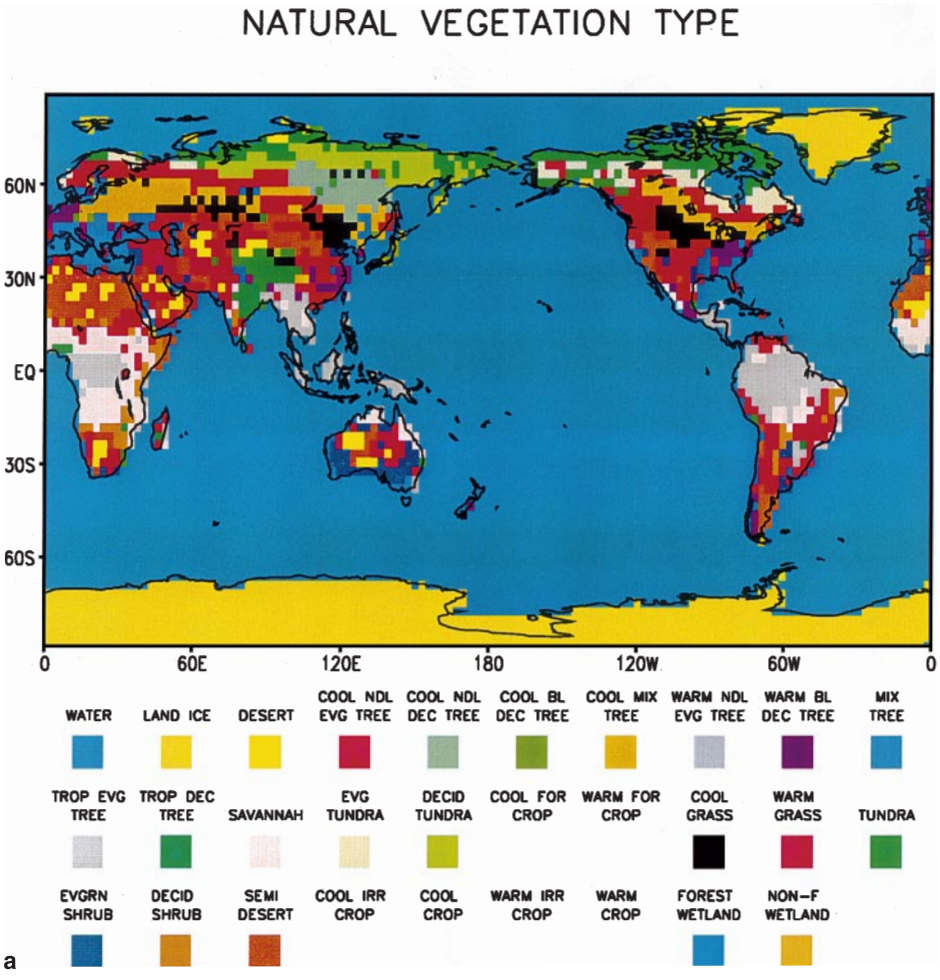

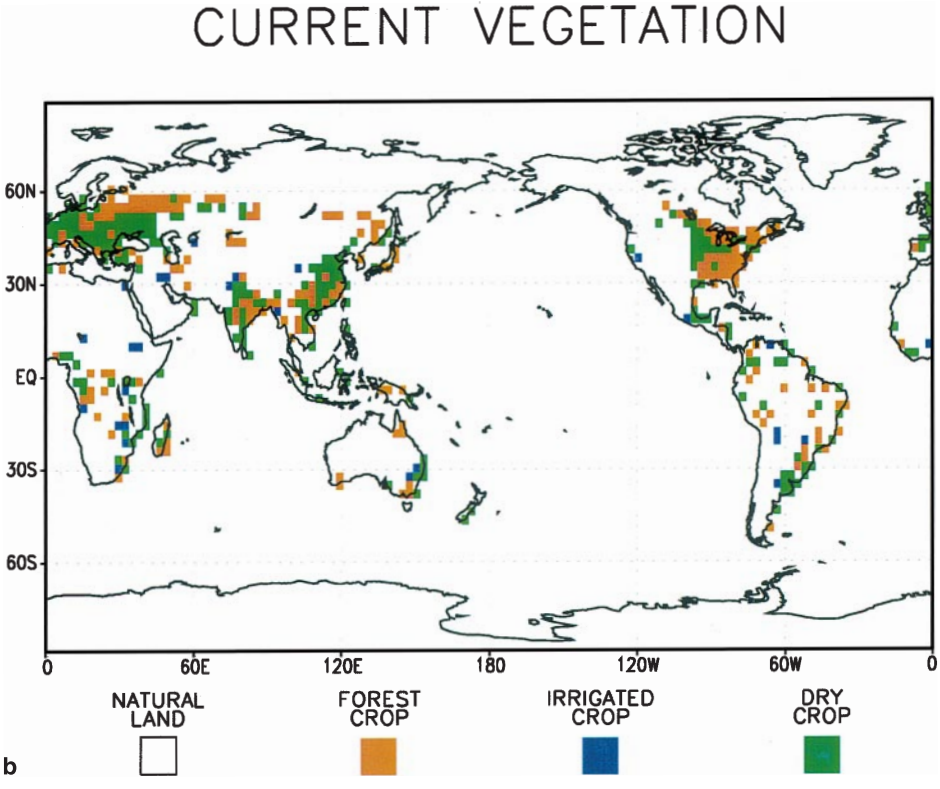

Fig. 1a, b Vegetation classifications for **a** natural vegetation and **b** current vegetation in regions where current and natural vegetation differ (i.e., anthropogenically disturbed regions in the current case)

between the two simulations resulted in changes in the fraction of the grid cell covered by vegetation, changes in soil moisture in irrigated regions, and differences in vegetation physical and physiological properties in the vegetated fraction.

4 Effects on tropical climate

With the exception of area averages, we present our results as differences in ten averaged Januaries between the current vegetation case and the natural vegetation case (current-natural) overlayed on a map of Student's t test statistic shaded at the 90 and 95%, 2-tailed, significance levels following Chervin and Schneider (1976).

Because our aim is to focus on the global effects of historic land use change, we do not perform a detailed regional analysis of the mechanism for changes in tropical convection. After the initial day of simulation, surface flux differences between the two cases were on the order of 5–10 W m^{-2} and occurred only over regions where direct land cover changes occurred (Chase 1999). After 10 years, surface heat flux anomalies (Fig. 2) are still associated with direct surface forcing from altered land cover though the largest heating anomalies results form adjustments by the atmosphere and large-scale circulation changes and occur in regions remote from direct forcings. For example, latent heat flux anomalies of nearly +40 W m^{-2} cover large portions of the tropical central and eastern Pacific. These are of similar magnitude to latent heat flux differences between observed warm and cold ENSO events (e.g., Wu and Newell 1998). Statistically significant changes in the distribution of surface heat fluxes (sensible and latent; Fig. 2a, b) resulting from changes in surface properties in the tropics are associated with shifts in tropical convection. Table 1 compares tropical (30°S–30°N) averages over regions where land cover differences exist between the two cases and so represent regions of direct forcing in these experiments. In regions of direct forcing, sensible heat fluxes increased, a warming of nearly 0.5 K occurred and precipitation decreased slightly under current vegetation. Decreased latent heat fluxes averaged over all tropical land surfaces (30°N–30°S) were positively correlated in space ($r = 0.45$; $P < 0.001$, Spearman's rank correlation coefficients) with decreased convective precipitation over tropical land surfaces (approximately 25% of convective precipitation in the latitude range 30°N–30°S occurred directly over land) and negatively correlated with increases in sensible heat fluxes ($r = 0.48$; $P < 0.001$) compatible with the assertion that tropical boundary layer equivalent potential temperature and therefore convection are strongly determined by boundary layer humidity (e.g., Brown and Bretherton 1998). Correlations with net radiation changes were insignificant ($P > 0.1$).

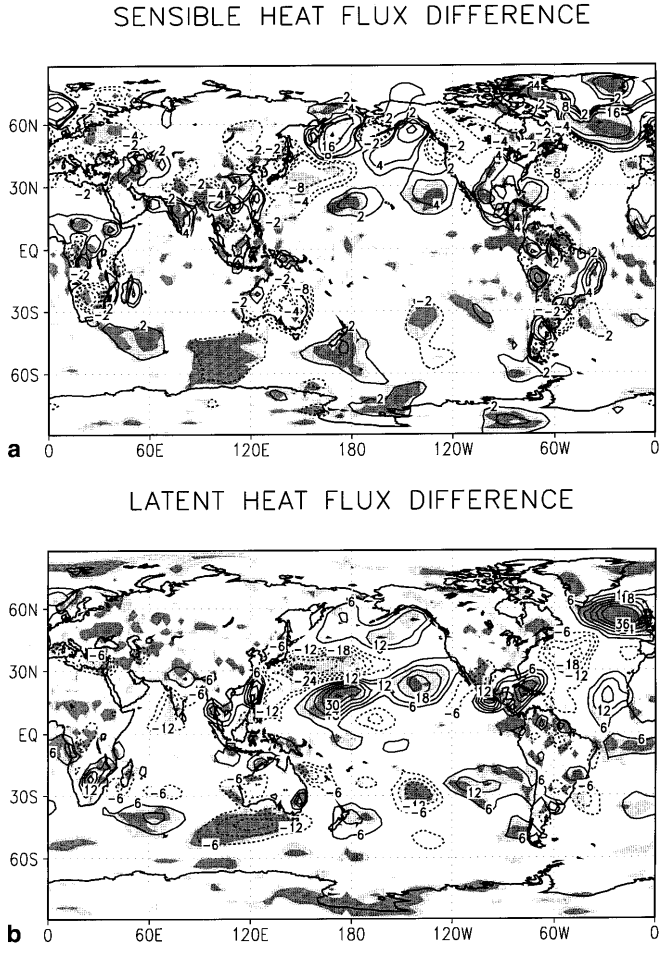

Fig. 2a, b Surface heat flux differences (current-natural) using a 9 point spatial filter for easier visibility. **a** Sensible heat flux (contours at 2, 4, 8, 16, 32 W m^{-2}); **b** latent heat flux (contours at 6 W m^{-2}). *Light shading* represents the 90% significance level for a *2-sided t*-test. *Dark shading* represents the 95% significance level

Figure 3a shows the distribution of the differences in convective precipitation and the associated t statistic map which indicate significant changes in precipitation of both sign over all the three tropical convective centers. Regional shifts in convection are apparent and of particular interest is the reduction in convective activity in the western Pacific and over the maritime continent while an increase in convective precipitation occurs in the central and eastern Pacific under current vegetation.

Figure 3b is a zonally averaged plot of convective precipitation from 45°S–45°N which shows that the effect of these changes was to diminish and move the intertropical convergence zone northward in the current vegetation case. The secondary maximum near 38°N was also diminished indicating a reduction in storm track activity.

Table 1 Selected fields averaged for 10 Januaries from 30°S–30°N and only over areas where land cover differences exist between the two cases

	Natural	Current	Difference
Sensible heat flux (W m^{-2})	36.34	42.90	+6.57
Latent heat flux (W m^{-2})	77.62	73.83	−3.80
Temperature (K)	292.39	292.83	+0.44
Precipitation (mm day^{-1})	3.78	3.75	−0.03

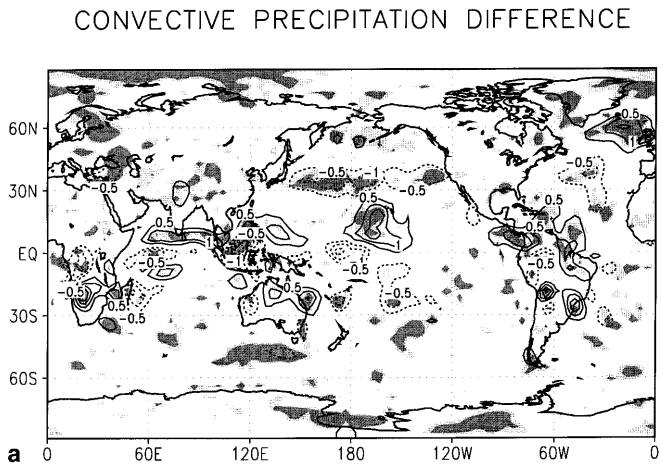

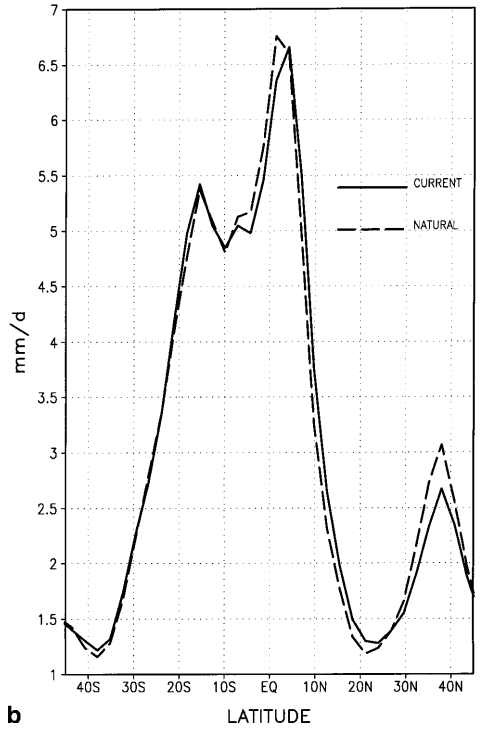

Fig. 3 a Convective precipitation differences (current-natural, contours at 0.5 mm/day) using a 9 point spatial filter for easier visibility. *Shaded regions* as in Fig. 3. **b** Comparison of the 45°N–45°S zonally averaged convective precipitation for the 2 cases

Tropical zonal circulations were also affected as seen in the differences in low-level (850 hPa) east-west winds (Fig. 4) which shows diminished easterlies over most of the central and eastern tropical Pacific (seen as positive wind anomalies because of the easterly flow).Though these changes are not statistically significant over the entire region, this reduction in easterlies is consistent with reduced convection over the western Pacific and Indonesia which acted to diminish the tropical zonal circulation. Because warm Southern Oscillation episodes are also characterized by decreased easterlies in these regions which are of similar magnitude to those simulated here (e.g., Philander 1990), our results indicate that

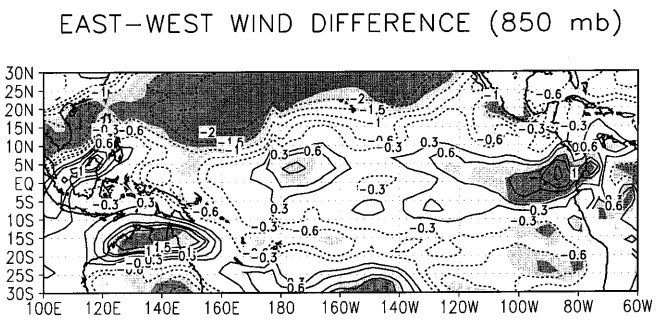

Fig. 4 Tropical Pacific east-west wind component difference at 850 hPa (contours by 0.3, 0.6, 1.0, 1.5, 2.0 m s^{-1}. *Shading* as in Fig. 3. Note: easterly winds are of negative sign so that decreased tropical easterlies are represented by positive wind anomalies

circulation changes resulting from tropical land use change may act, to first order, to enhance the magnitude, frequency and duration of warm Southern Oscillation episodes and to diminish cold episodes. This, in some ways, is consistent with the results of Lau and Bua (1998) who found enhanced ENSO teleconnection patterns when interactive land surfaces, particularly in east Asia and Indochina, were included in model simulations.

5 Effects on higher latitudes

Changes in large-scale circulations as a result of observed land use change are also highly significant. The kinetic energy per unit mass (*KE*) associated with the divergent components (U_χ and V_χ) of the wind, where $KE = (U_\chi^2 + V_\chi^2)/2$ can be used as a measure of tropical high-level outflow and its influence on the extratropical circulation. The difference in this quantity at 200 hPa (Fig. 5a) shows a significant decrease in divergent high-level tropical outflow in all three major tropical heating centers in the current vegetation case. By far the largest effect is in southeast Asia/Indonesia and the western Pacific. In the zonal average (Fig. 5b), 200 hPa divergent kinetic energy is reduced everywhere but particularly in the tropical maximum which is a reflection of both a diminished global meridional circulation and diminished tropical zonal circulations in the current vegetation case. Because divergent *KE* is quickly converted to the rotational *KE* associated with the mid-latitude jet (Wiin-Nielsen and Chen 1993), there is considerably less energy available to directly feed the jet in the current vegetation case.

Differences in the mean meridional stream function are shown in Fig. 6. The stream function under current vegetation is also shown for comparison (Fig. 6a). The dipole of negative values in the 10-year difference field (Fig. 6b) from approximately 5°S–10°N and positive values from 10°–40°N reflect a northward shift of the winter hemisphere Hadley cell under current vegetation. The maximum mass flux in this case is 19.64×10^{10} g m^{-2} s^{-1} while under natural vegetation the maximum value is 19.77×10^{10} g m^{-2} s^{-1}. The negative values from

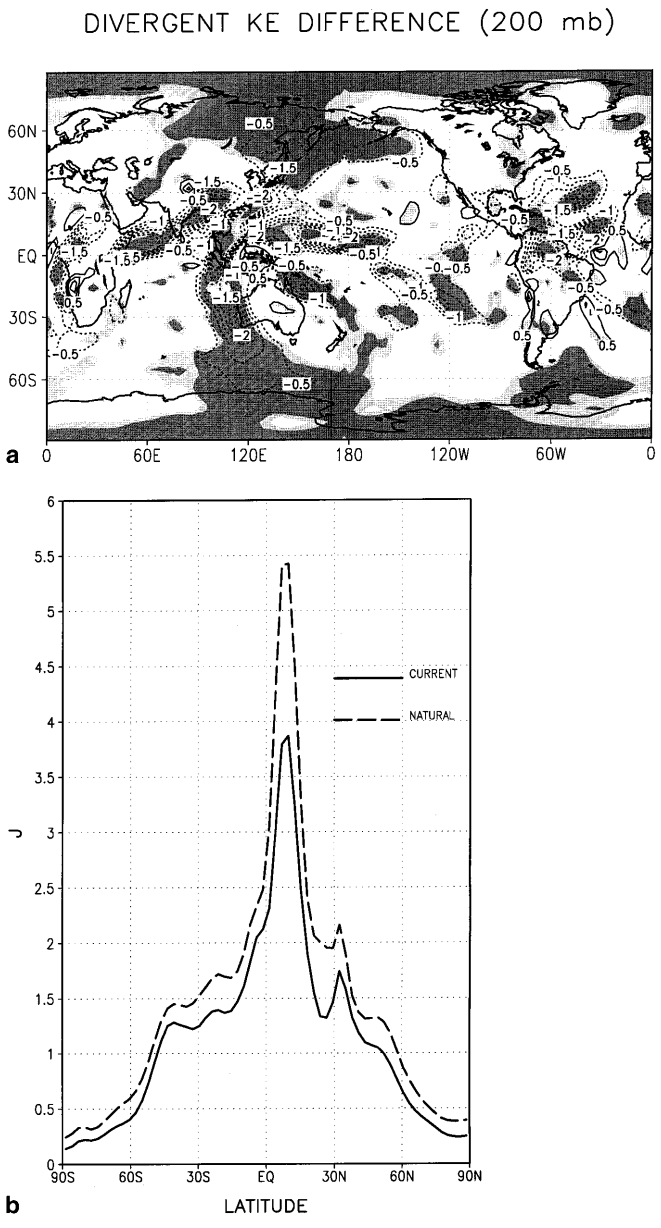

Fig. 5 a Divergent wind kinetic energy (*KE*) difference per unit mass at 200 hPa, (contours = 0.5 J). *Shaded regions* as in Fig. 3. **b** Comparison of zonally averaged 200 hPa *KE* for the two cases

40°–60°N indicate an increased Ferrel cell circulation under current vegetation. Figure 6c shows a difference in mean meridional streamfunction for the last 5 years of the simulation only. That the overall pattern is similar to the 10-year difference is an indication of the robustness of the change in planetary circulation.

Changes in tropical convection not only reduced the the intensity of the mean meridional circulation and of the upper-level divergent tropical outflow under current vegetation, anomolous vorticity forcings were also generated which appear to affect high Northern Hemisphere latitudes. Starting with the barotropic vorticity (ζ) equation and defining a divergent ($\mathbf{V}_\chi$) and rotational ($\mathbf{V}_\psi$) component of the wind, a vorticity equation can be written in the form (Sardeshmukh and Hoskins 1988; James 1994):

$$\frac{\partial \zeta}{\partial t} + \mathbf{V}_\psi \cdot \nabla\zeta = -\zeta(\nabla \cdot \mathbf{V}) - \mathbf{V}_\chi \cdot \nabla\zeta = -\nabla \cdot (\mathbf{V}_\chi \zeta). \quad (1)$$

The forcing term on the far righthand side of Eq. (1) is a function solely of the divergent component of the wind (refer to the divergent *KE* in Figs. (6a, b) and the vorticity gradient. Differences in this forcing term (known as the Rossby source term) between the current and natural vegetation scenarios at 200 hPa are presented in Fig. 7. Significant anomalies of both sign are generated in all three tropical heating centers though the strongest and most widespread effect occurs in southeast Asia and to its south and east. The strongest Rossby source anomalies in the region of southeast Asia central Pacific occur in locations of westerlies which allows for the possibility of propagation to higher latitudes, thereby potentially affecting mid-latitude weather and climate regimes as discussed in the introduction.

The possible connection between anomalous Rossby wave forcing in the western and central Pacific and the higher northern latitudes can be clarified with a correlation analysis of height data. A correlation in the January average 500 hPa height difference fields between the natural and current vegetation simulation with the differences at the base point 21°N–158°W (Fig. 8) (a center of action for tropical Pacific convection differences and a region of westerlies at all tropical latitudes) reveals a teleconnection pattern which affects the entire Northern Hemisphere and is similar in spatial structure to the Tropical Northern Hemisphere (TNH) pattern described in studies examining extratropical connection to El Niño (e.g., Livezey and Mo 1987). These correlations are significant at the 5% level at most of the amplitude extrema throughout the hemisphere.

Significant changes in large-scale, high-latitude Northern Hemisphere flow were generated as a result of the historic changes land cover and are attributable to changes in tropical convection discussed. The differences in east-west winds at 200 hPa (Fig. 9a) shows a prominent northward shift in the mid-latitude jet stream over most of the globe under the current vegetation scenario. This shift is most apparent in the northern Pacific. Zonal averages of the 200 hPa east-west wind (not shown) display this northerly shift and a decrease in the maximum magnitude of the jet core in the current case by approximately 5 m s^{-1}; a decrease of more than 10%. The northern shift and decreased magnitude of the mid-latitude jet (a feature noted in the global land cover change experiment of Chase et al. 1996 and the desertification experiment of Dirmeyer and Shukla 1996) are consistent with the decreased upper-level tropical outflow in the current vegetation case which can provide less direct energy to the jet (Fig. 6), and with a decreased and more northerly temperature gradient maximum in the current case. This change in gradient can be seen in the zonally averaged north-south gradient in 200 hPa heights in the Northern Hemisphere (a measure of the

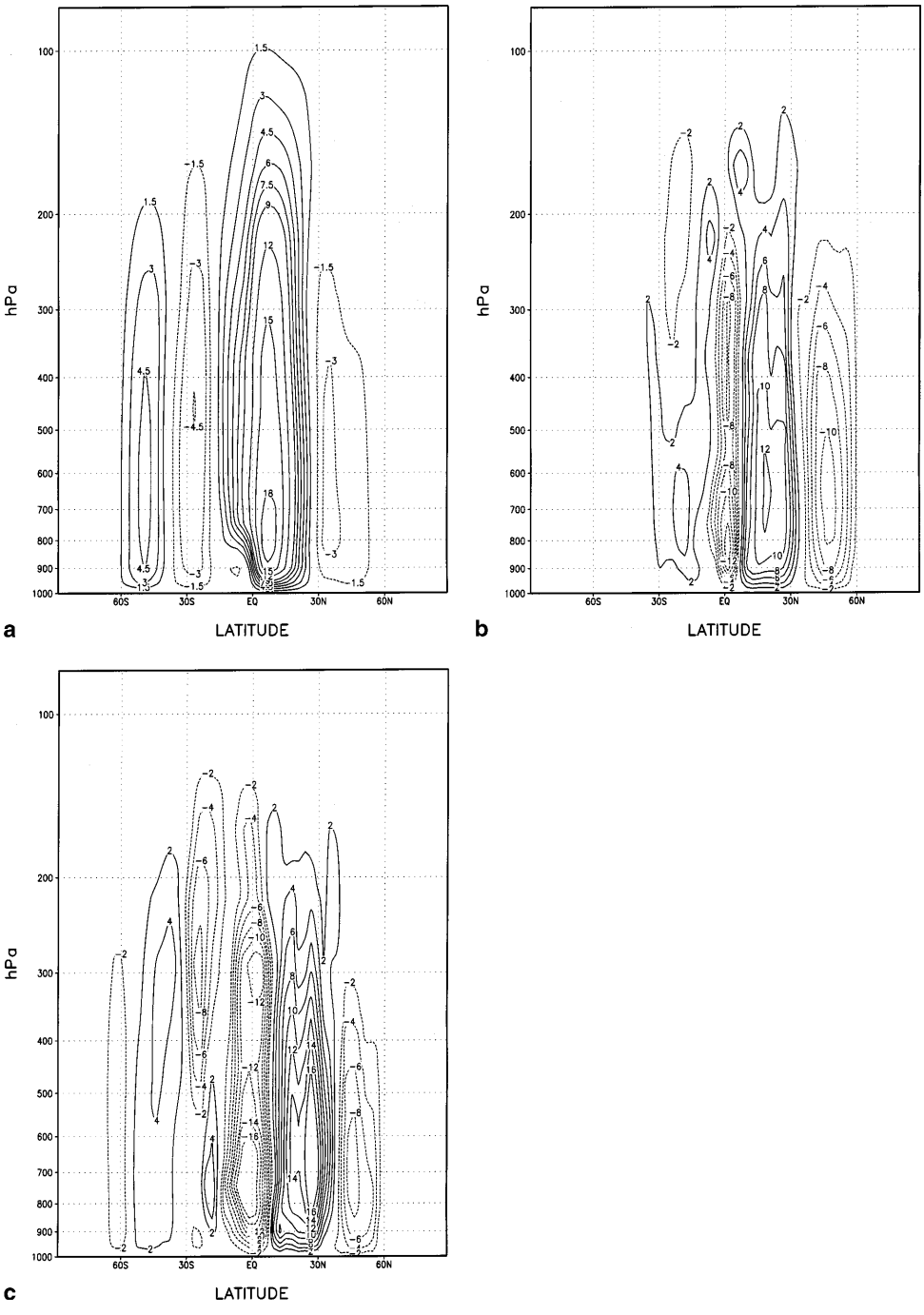

Fig. 6a–c Mean meridional stream function for **a** current vegetation (contours at 1×10^{11} kg s^{-1}), **b** 10 year January difference (current-natural; 1×10^{10} kg s^{-1}), and **c** last 5-year January difference (current-natural; 1×10^{10} kg s^{-1})

vertically averaged horizontal temperature gradient, Fig, 9b) which shows a northerly shift and weakening in the zone of maximum baroclinicity in the current vegetation case. It should be noted that changes in the mean flow such as those described will also affect the propagation characteristics of and interact with, waves superimposed on that flow (e.g., Rasmussen and Wallace 1983; Kang 1990; Ting et al. 1996) which introduces yet another source of variability between current and natural vegetation scenarios. Finally, under current vegetation, zonally averaged temporal variability, measured here as the monthly-averaged standard deviation of daily 500 hPa heights (Fig. 10) in jet stream regions was reduced as would be expected from diminished baroclinicity.

Figure 11 shows near surface air temperature difference between current and natural vegetation. Significant changes in temperature are associated with all tropical land masses and many higher latitude regions. In the Northern Hemisphere, a wave number 3 pattern of warming and cooling centers is apparent. Warming occurs on most land surfaces under current vegetation and is centered in temperate and eastern boreal North America, southern Asia, and central Europe. Cooling

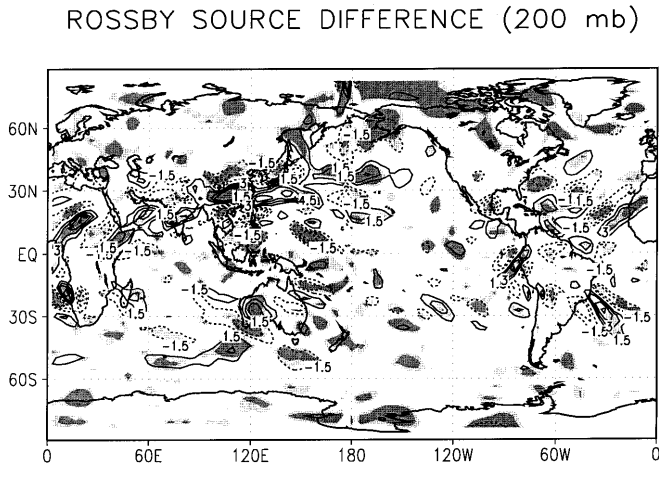

Fig. 7 Rossby source term differences (current-natural) $\times 10^{10}$ (contours at 1.5 s^{-2}). *Shaded regions* as in Fig. 3

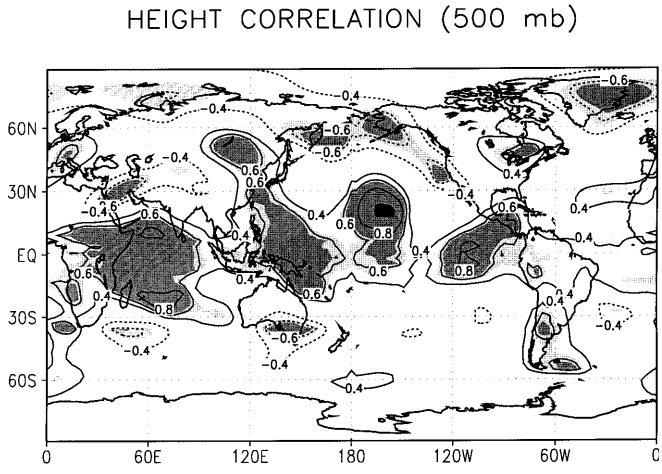

Fig. 8 Correlation of differences in 500 hPa height field with difference at 21°N and 158°W. Contours at 0.4, 0.6, 0.8. *Blackened region* in central Pacific represents the region of near perfect correlation. *Shading* as in Fig. 3 but for significance of correlation

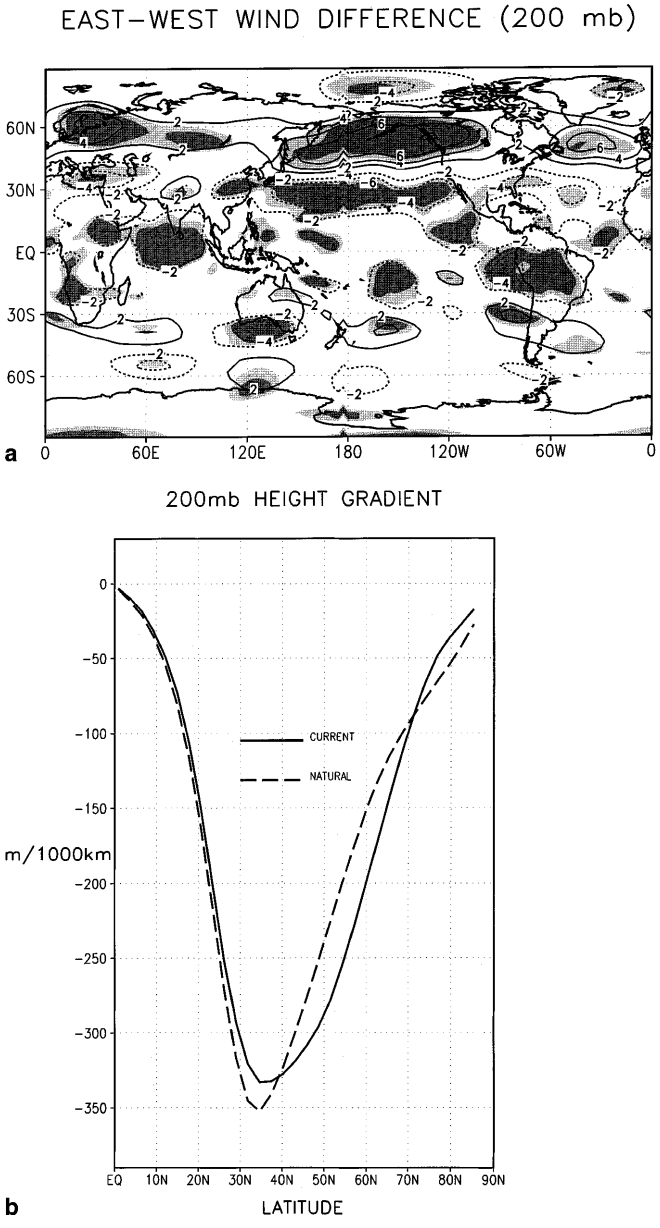

Fig. 9 **a** Difference in 200 hPa east-west wind (current-natural), contours are 2 m s^{-1}. *Shaded regions* as in Fig. 3. **b** Comparison of north-south derivative of zonally averaged 200 hPa heights (d(Z200)/dy) in Northern Hemisphere

centers include the western Arctic (including the North Pacific and Alaska), Greenland, and the North Atlantic and central Asia. Temperature differences in Fig. 11 represent the combined effects of changes in the basic zonally averaged circulation, differences in waves superimposed on that basic state, and also differences in local forcing due to changes in snow cover. Most of the surface temperature response is due to changes in large-scale circulation. The spatial correlation coefficient in latitudes from 30°–60°N between differences in surface temperature and differences in 200 hPa heights (Fig. 12a) is 0.72. Correlations between differences in albedo (Fig. 12b) which results mostly from changes in snowcover is 0.06. This indicates that, overall, and opposite to expectation, should albedo be a primary forcing, increased albedo is weakly associated with increased temperature and again points out the importance of changes in the large-scale circulation in forcing the surface temperature differences. Changes in surface albedo appear to be having a positive feedback effect in some regions on the surface temperature field, however. The large warming in western Europe is associated with decreased albedo and increased 200 hPa heights while a cooling in central Asia is associated with increased albedo and decreased heights. Warming in northeastern Canada is also associated with decreased albedo and increased heights.

The average temperature changes from 30°N–90°N is +0.29 °C over land which is of the same magnitude as observed in the surface record in recent decades (e.g., Pielke et al. 1998a, b). Globally, temperatures warmed by 0.05 °C in the current case. It should be

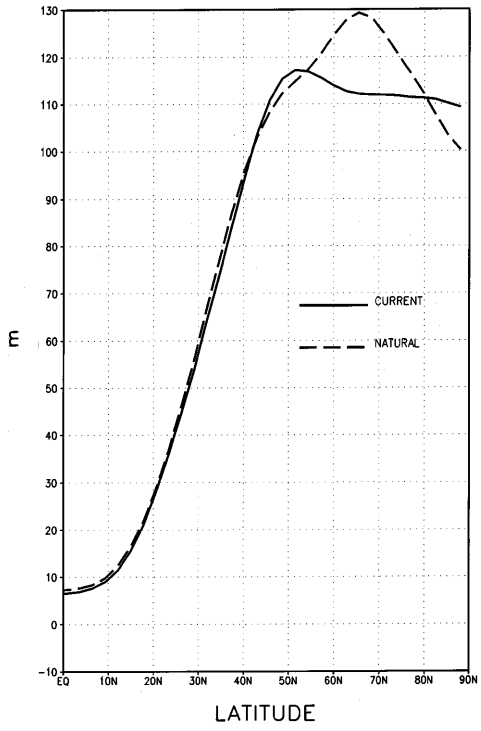

Fig. 10 Comparison of Northern Hemisphere zonally and monthly averaged daily standard deviation in 500 hPa heights

noted that the atmospheric temperatures over ocean and sea ice are limited by the imposed surface temperatures in those regions. This warming of Northern Hemisphere land surfaces is associated with weakened equatorward, low-level, winter monsoon flow which allowed the ITCZ to occupy its more northerly position in the current vegetation case (Fig. 3b). These temperature differences, which are a result of large-scale circulation changes and which are statistically significant at 5 of the 6 cooling/warming centers, are interesting given observed, Northern Hemisphere, winter climate trends which are discussed in section 6.

6 Comparison with observed circulation changes

Because a fully dynamic coupling between all atmospheric, oceanic, and land surface processes is not achieved in these simulations, it is necessary to interpret our results as sensitivities within a simplified system. Only if land surface changes were dominant or the couplings with other components of the climate system were weak or on longer time scales, would we expect to see an immediately obvious correspondence between observational evidence of the effects of land use change and model results. In this section we look for possible signals corresponding to the model simulations in reported observations recognizing these limitations.

The January warming in the current vegetation case simulated over much of the land area in the Northern Hemisphere including most of North America, Europe,

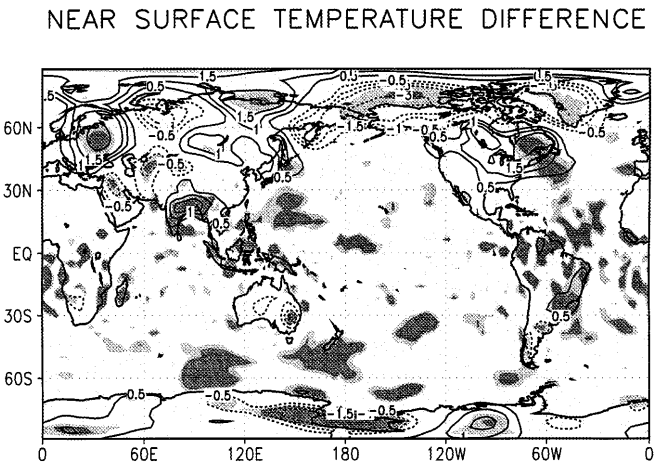

Fig. 11 Difference in near-surface air temperature (current-natural) using a 9-point spatial filter for easier visibility. Contours at 0.5, 1.0, 1.5, and 3.0 °C. *Shaded regions* as in Fig. 3

and parts of Siberia as well as the cooling over ocean areas is, in some ways, consistent with observational evidence which notes recently increased surface air temperatures over land in Northern Hemisphere winter, while oceans appear to be cooling (e.g., Wallace et al. 1996; Hurrell 1996; Palecki and Leathers 1993). These authors relate these temperature trends to anomalous circulations associated primarily with the Pacific North America pattern (PNA) and the North Atlantic Oscillation (NAO) though other recognized modes of variability such as the tropical Northern Hemisphere (TNH) pattern (discussed in Sect. 5) are also implicated.

Anomalous circulations in the northern Pacific have been associated with changes in sea surface temperature forcing of tropical convection and seem to be related to recent increases in the duration and magnitude of EI Niño events (Trenberth and Hurrell 1994), an effect we have no representation of in the present simulations due to prescribed, annually cycling SSTs. The observed effects of this increase in El Niño events include a heightened tropical hydrological cycle, an amplification and southerly movement of the mid-latitude Northern Hemisphere storm tracks and an eastward movement and deepening of the Aleutian low. An index of these observed changes (the NP index = area-averaged surface pressure from 30–65°N and from 160°E–140°W; Trenberth and Hurrell 1994) shows a recent increase in the magnitude of this index of 2.2 hPa from the long-term average.

Our simulated circulation changes in the extratropical northern Pacific as measured by the NP index is a decrease of nearly 1.5 hPa and shows decreased tropical outflow and a northerly movement of the jet. These effects are opposite in sign to those observed and are consistent with a less active tropical hydrologic cycle in the current vegetation case. This is not surprising because our simulations include no representation of the observed, more frequent, warm eastern and central

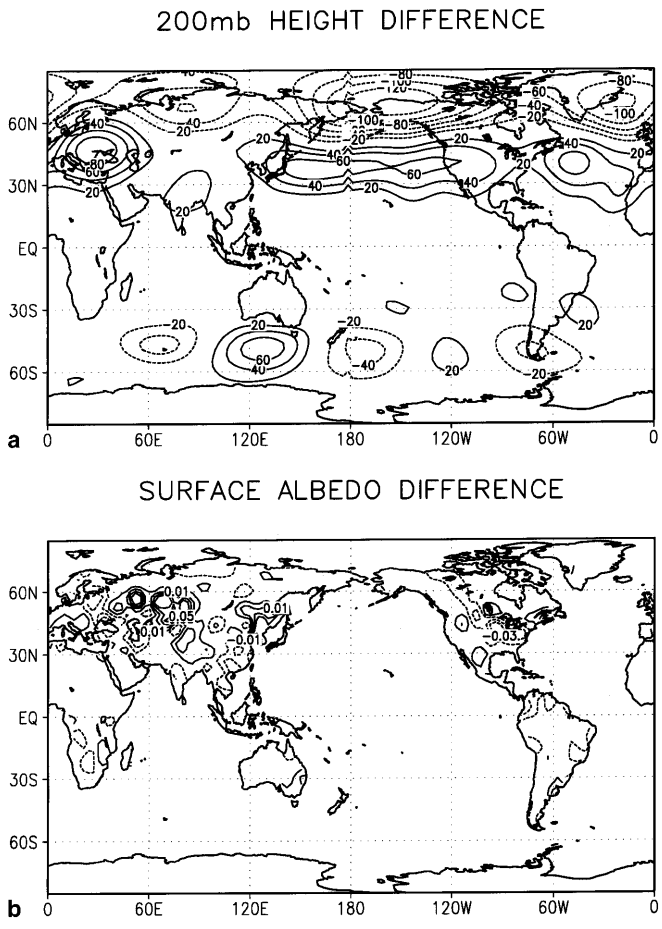

Fig. 12 **a** The 200 hPa height difference (current-natural), contours at 20 m and **b** surface albedo difference (current-natural) using 9 point spatial filter. Contours at 0.01, 0.03, 0.05, 0.07 (units are fractional change; i.e., 0.01 = 1.0% change in albedo

tropical Pacific ocean temperatures associated with increased El Niño events which appear to have a strong relationship with observed atmospheric circulation changes in the Northern Pacific (Ponte and Rosen 1994; Kumar et al. 1994; Yulaeva and Wallace 1994). However, our simulations indicate decreased easterlies over much of the tropical Pacific Basin under current vegetation which, to first order, might act to amplify the magnitude and frequency of El Niño events (e.g., Trenberth and Hoar 1996).

As a result of the current phase of the North Atlantic Oscillation (NAO) the North Atlantic has also experienced large-scale circulation changes during northern winter which have resulted in strong warming over land in western Europe and Siberia. These very strong regional warming trends make up a significant portion of the observed area-average surface Northern Hemisphere and global warming trends. An index of the phase of NAO which compares surface pressure between Lisbon, Portugal and Stykkisholmur, Iceland shows the NAO in a positive phase since 1980 with values of the index between +1 to +3 hPa (Hurrell 1996). A calculation of the same index in our simulation between the two vegetation cases gives a +3 hPa value when going from natural to current vegetation. No strong connection between tropical SST and large-scale circulation changes in the Atlantic (e.g., Kumar et al. 1994) exists. Our results suggest the possibility of an interaction between circulations driven by land cover change and Atlantic climate anomalies.

7 Discussion and conclusions

Land use changes, particularly in the tropics, should be expected to have global effects. Unlike the fluctuations associated with opposing phases of ENSO, the direct surface heating anomalies and subsequent changes in circulation associated with land use change are essentially permanent. To investigate the hypothesis that observed land use change can have effects at global scales, we examined 10 years of modeled equilibrium January climate differences between simulations which were forced at the surface by: (a) a spatially realistic depiction of the current land surface, and (b) an estimate of natural potential vegetation in equilibrium with current climate.

Wu and Newell (1998) concluded that SST variations in the tropical Eastern-Pacific have three unique properties that allow the tropical ocean to influence the atmosphere effectively: large magnitude, long persistence, and spatial coherence. Both direct land use changes and resulting circulation changes in the tropics have similar properties which, in our simulations, resulted in climate anomalies at higher latitudes. The largest climatic changes were not limited to the region of direct land use change indicating that atmospheric and feedbacks within the tropics and teleconnections from the tropics to higher latitudes were more important than the direct forcing in this case.

Differences between the current and natural vegetation scenarios included a zonally averaged northward shift and decreased magnitude of tropical convection as well as east-west shifts in tropical convective precipitation particularly in the Pacific basin and the maritime continent. The changes in tropical convection resulted in a diminished Hadley cell circulation and reduced high-level outflow from the tropics, less direct conversion of divergent kinetic energy to the rotational kinetic energy of the mid-latitude jet which contributed to a northerly shift and a reduction in peak magnitude of the zonally averaged jet. This is consistent with a reduction in the associated meridional temperature gradient. The shift in pattern and strength of tropical convection combined with changes in the zonally averaged basic state also generated anomalous vorticity sources under the current vegetation scenario which appear to have affected climate at high latitudes throughout the Northern Hemisphere. Shifts in tropical convection also produced reduced easterlies over much of the tropical Pacific basin and a central Pacific positive convective anomaly suggesting further high-latitude effects could arise through a

positive interaction with the warm phase of ENSO. These effects are of greatest magnitude in the regions of Southeast Asia and the maritime continent which suggests that land use change in these areas is of considerable importance to the study of global climate; a conclusion also reached by Lau and Bua (1998). That our vegetation distribution reflects more deforestation in this region than most others may explain, in part, why our extra-tropical results are more clearly evident relative to other GCM land cover change experiments.

A previous simulation (Chase et al. 1996) using a GCM with the same dynamical framework through with differing physical parameterizations from the present work produced similar effects (including a northern shift of the ITCZ and a northward movement and weakening of the zonally averaged mid-latitude jet) by simply realistically altering the amount of green leaf area in regions affected by human activity. This indicates that vegetative effects on tropical convection may be controlled by physiological processes as much as by physical factors such as albedo and roughness length. This view is given support by Kleidon and Heimann (1998) who found that rooting depth, a biological control on transpiration and soil moisture availability, was a significant factor in the production of latent heat and temperature in tropical regions and therefore affected tropical convection.

These results also suggest that teleconnection patterns due to anthropogenic land cover changes which have already occurred are capable of affecting the temperature and precipitation distributions worldwide and may have already done so. Such effects are traditionally unaccounted for in global climate trend analyses (e.g., North and Stevens 1998) but growing evidence indicates that these effects may have to be accounted for in climate change monitoring efforts (e.g., Pielke et al. 1998a, b and references therein) necessitating further examination of their scope and significance.

The issue of the overall effect of prescribed SSTs on the simulation results is an important remaining question. There is no reason to believe a priori that the inclusion of an interactive ocean component would result in either a damped or enhanced signal due to landcover changes. Bonan (1992) found that the inclusion of an ocean model significantly enhanced the northern winter climate signal caused by boreal deforestation particularly at higher latitudes. This could be an indication that the non-interactive ocean in the present simulations artificially accentuates tropical effects relative to the effects of direct land cover and snow cover changes at high latitudes. There is some indication, however, that an interactive ocean would also enhance the tropical effects through an interaction with ENSO as discussed in Sect. 4.

Finally, while we do not consider this, or any, climate simulation model to be comprehensive enough to provide reliable climate predictions (e.g., because of the lack of a dynamical ocean component in the present case, Campbell et al. 1995, but also because of imprecise depictions of vegetation properties and the nonlinear feedbacks between these processes), some observed trends in tropical and Northern Hemisphere winter circulations are, in part, suggestive of a global response due to land use change. While the spatial pattern of Northern Hemisphere warming is not identical in our simulations to that observed, the large-scale circulation changes responsible for it are sufficiently similar to those thought responsible for the observed warming to suggest an interaction. Additionally, the observed pattern of more intense and longer warm ENSO events at the expense of cold ENSO events which is implicated in much of the observed higher latitude winter warming is implicitly simulated by decreased easterlies in the tropical Pacific and a positive convective anomaly in the central Pacific which appears to affect high latitudes as a result of changed land cover. This result highlights a further avenue for investigation. These patterns of recently warming surface temperatures over Northern Hemisphere land areas resulting solely from dynamical atmospheric shifts have been difficult to associate convincingly with global CO_2 warming (e.g., Plantico et al. 1990; Jones 1988; Hurrell 1996) and our results suggest that global land cover change may already have had an important and measurable effect on the observed global climate state.

Acknowledgements The authors acknowledge support from the National Park Service (NPS) and the National Biological Survey (NBS) Grants CEGR-R92-0193 and COLR-R92-0204, the United States Geological Survey (USGS) Grant 1434-94-A-01275, Environmental Protection Agency (EPA) Grant R824993-01-0, and the National Oceanic and Atmospheric Administration (NOAA) grant NA36GP0378. Additional support was received from the University Corporation for Atmospheric Research Climate Systems Modeling Program contract UCAR S9361 (funded by the National Science Foundation, NSF). The National Center for Atmospheric Research in sponsored by NSF and is acknowledged for supplying the model and computational cycles for this work. We thank Dr. John Knaff, Dallas McDonald, Tara Pielke and two anonymous reviewers for their helpful comments.

References

Berbery EH, Nogués-Paegle J (1993) Intraseasonal interactions between the tropics and extratropics in the Southern Hemisphere. J Atmos Sci 50:1950–1965

Bjerknes J (1969) Atmospheric teleconnections from the equatorial Pacific. Mon Weather Rev 97:163–172

Bonan GB (1996) A land surface model (LSM version 1.0) for ecological, hydrological and atmospheric studies: technical description and users guide. NCAR Technical Note NCAR/TN-417+STR

Bonan GB, Pollard D, Thompson SL (1992) Effects of boreal forest vegetation on global climate. Nature 359:716

Brown RG, Bretherton CS (1998) A test of the strict quasi-equilibrium theory on long time and space scales. J Atmos Sci 54:624–638

Burde GI, Zangvil A (1996) Estimating the role of local evaporation in precipitation in two dimensions. J Clim 9:1328–1338

Campbell GC, Kittel TGF, Meehl GA, Washington WM (1995) Low-frequency variability and CO_2 transient climate change. Part 2: EOF analysis of CO_2 and model-configuration sensitivity. Global Planet Change 10:201–216

Chase TN (1999) The role of historical land-cover changes as a mechanism for global and regional climate change. Ph D Dissertation. Colorado State University. Ft. Collins, CO, USA

Chase TN, Pielke, RA, Kittel TGF, Nemani R, Running SW (1996) The sensitivity of a general circulation model to large-scale vegetation changes. J Geophys Res 101:7393–7408

Chen TC, Tzeng RY, Van Loon H (1988) A study of the maintenance of the winter subtropical jet streams in the Northern Hemisphere. Tellus 40A:392–397

Chervin RM, Schneider SH (1976) On determining the statistical significance of climate experiments with general circulation models. J Atmos Sci 33:405–412

Claussen M (1998) On multiple solutions of the atmosphere-vegetation system in present-day climate. Global Change Biol (in press)

Copeland JH (1995) Ph D Dissertation: Impact of soil moisture and vegetation distribution on July 1989 climate using a regional climate model. Department of Atmospheric Science, Colorado State University, 124 pp

Dickinson RE, Kennedy PJ (1992) Impacts on regional climate of Amazonian deforestation. J Geophys Res Lett 19:1947–1950

Dirmeyer PA, Shukla J (1996) The effect on regional and global climate of expansion of the world's deserts. Q J R Meteorol Soc 122:451–482

Eltahir EAB (1996) Role of vegetation in sustaining large-scale atmospheric circulation in the tropics. J Geophys Res 101:4255–4268

Eltahir EAB (1998) A soil moisture-rainfall feedback mechanism 1. Theory and observations. Water Resources Res 34:765–776

Geisler JE, Blackmon ML, Bates GT, Munoz S (1985) Sensitivity of January climate response to the magnitude and position of equatorial Pacific sea surface temperature anomalies. J Atmos Sci 42:1037–1049

Hack JJ (1994) Parameterization of moist convection in the National Center for Atmospheric Research Community Climate Model (CCM2). J Geophys Res 99:5551–5568

Hack JJ, Kiehl JT, Hurrell JW (1998) The hydrologic and thermodynamic characteristics of the NCAR CCM3. J Clim 11:1179–1206

Hoerling MP, Ting M (1994) Organization of extratropical transients during El Niño. J Clim 7:745–766

Hurrell JW (1996) Influence of variations in extratropical wintertimes teleconnections on Northern Hemisphere temperature. Geophys Res Lett 23:665–668

James IN (1994) Introduction to circulating atmospheres. Cambridge University Press, Cambridge, UK, pp 266–268

Jones PD (1988) Hemispheric surface air temperature variations: recent trends and an update to 1987. J Clim 1:654–660

Kang I-S (1990) Influence of zonal mean flow change on stationary wave fluctuations. J Atmos Sci 47:141–147

Kiehl JT. Boville B, Briegleb B, Hack J, Rasch P, Williamson D (1996) Description of the NCAR Community Climate Model (CCM3). NCAR Technical Note NCAR/TN-420 + STR, Boulder, Colorado, USA

Kleidon A, Heimann M (1998) Optimized rooting depth and its impacts on simulated climate of an atmospheric general circulation model. Geophys Res Lett 25:345–348

Krishnamurti TN (1961) The subtropical jet stream of winter. J Meterol 18:172–191

Krueger, AF, Winstons JS (1973). A comparison of the flow over the tropics during two contrasting flow regimes. J Atmos Sci 31:358–369

Kumar A, Leetmaa A, Ji M (1994) Simulations of atmospheric variability induced by sea surface temperatures and implications for global warming. Science 266:632–634

Lau K-M, Bua W (1998). Mechanisms of monsoon-Southern Oscillation coupling: insights from GCM experiments. Clim Dyn 14:759–779

Lettau H, Lettau K, Molion LCB (1979) Amazonia's hydrologic cycle and the role of atmospheric recycling in assessing deforestation effects. Mon Weather Rev 107:227–237

Livezey RE, Mo KC (1987) Tropical-extratropical teleconnections during Northern Hemi-sphere winter. Part II: relationship between monthly mean Northern Hemisphere circulation patterns and proxies for tropical convection. Mon Weather Rev 115:3115–3132

Matthews E (1983) Global vegetation and land use: new high resolution data bases for climate studies. J Clim Appl Meteorol 22:474–487

McGuffie K, Henderson-Sellers A, Zhang H, Durbridge TB, Pitman AJ (1995) Global climate sensitivity to tropical deforestation. Global Plane Change 10:97–128

Mintz Y (1984) The sensitivity of numerically simulated climates to land-surface boundary conditions. In: Houghton J. (ed), The global climate pp 79–105, Cambridge University Press, 233 pp. Cambridge

Neilson RP, Marks D (1994) A global perspective of regional vegetation and hydrologic sensitivities from climatic change. J Veget Sci 5:715–730

Nemani RR, Running SW (1989) Testing a theoretical climate-soil-leaf area hydrologic equilibrium of forests using a satellite data and ecosystem simulation. Agric Forest Meteorol 44:245–260

Nemani RR, Running SW, Pielke RA, Chase TN (1996) Global vegetation cover changes from coarse resolution satellite data. J Geophys Res 101:7157–7162

Nobre CA, Sellers PJ, Shukla J (1991) Amazonia deforestation and regional climate change. J Clim 4:957–988

North GR, Stevens MJ (1998) Detecting climate signals in the surface temperature record. J Clim 11:563–577

Olson JS, Watts JA, Allison LJ (1983) Carbon in live vegetation of major world ecosystems. ORNL-5862. Oak Ridge National Laboratory, Oak Ridge, TN, USA

Oort AH, Yienger JJ (1996) Observed interannual variability in the Hadley circulation and its connection to ENSO. J Clim 9:2751–2767

Palecki MA, Leathers DJ (1993) Northern Hemisphere extratropical circulation anomalies and recent January land surface temperature trends. Geophys Res Lett 20:819–822

Philander SG (1990) El Nino, La Nina and the Southern Oscillation. Academic Press. San Diego, USA

Pielke RA, Lee TJ, Copeland JH, Eastman JL, Ziegler CL, Finley CA (1997) Use of USGS-provided data to improve weather and climate simulations. Ecol Appl 7:3–21

Pielke RA, Eastman JL, Chase TN, Knaff JA, Kittel TGF (1998a) 1973–1996 trends in depth-averaged tropospheric temperature. J Geophys Res 103:16 927–16 933

Pielke RA, Eastman JL, Chase TN, Knaff JA, Kittel TGF (1998b) Errata to 1973–1996 trends in depth-averaged tropospheric temperature. J Geophys Res 103:28909–28911

Polcher J, Laval K (1994) A statistical study of regional impact of deforestation on climate of the LMD-GCM. Clim Dyn 10:205–219

Plantico MS, Karl TR, Kukla G, Gavin J (1990) Is recent climate change across the United States related to rising levels of anthropogenic greenhouse gases? J Geophys Res 95:16 617–16 636

Ponte RM, Rosen RD (1994) Angular momentum and torques in a simulation of the atmosphere's response to the 1982–83 El Niño. J Clim 7:538–550

Rasmussen EM, Wallace JM (1983) Meteorological aspects of the El Niño/southern oscillation. Science 222:1195–1202

Sagan C, Toon OB, Pollack JB (1979) Anthropogenic climate changes and the Earth's climate. Science 206:1363–1368

Sardeshmukh PD, Hoskins BJ (1988) The generation of global rotational flow by steady idealized tropical divergence. J Atmos Sci 45:1228–1251

Sellers PJ, Bounana L, Collatz GJ, Randall DA, Dazlich DA, Los SO, Berry JA, Fung I, Tucker CJ, Filed CB, Jensen TG (1996) Comparison of radiative and physiological effects of doubled atmospheric CO_2 on climate. Science 271:1402–1406

Stohlgren TJ, Chase TN, Pielke RA, Kittel TGF, Baron J (1998) Evidence that local and land use practices influence regional climate and vegetation patterns in adjacent natural areas. Global change Biol 4:495–504

Sud YC, Walker GK, Kim JH, Liston GE, Sellers PJ, Lau WKM (1996) Biogeophysical cosequences of a tropical deforestation scenario: a GCM simulation. J Clim 9:3225–3247

Tiedtke M (1984) The effect of penetrative cumulus convection on the large-scale flow in a general circulation model. Beitr Phys Atmos 57:216–224

Ting M, Hoerling MP, Xu T, Kumar A (1996) Northern Hemisphere teleconnection patterns during extreme phases of the zonal mean circulation. J Clim 9:2614-2633

Trenberth KE, Hurrell JW (1994) Decadal atmosphere-ocean variations in the Pacific. Clim Dyn 9:303–319

Trenberth KE, Hoar TJ (1996) El Niño Southern oscillation event: longest on record. Geophys Res Lett 23:57–60

Tribbia JJ (1991) The rudimentary theory of atmospheric teleconnections associated with ENSO. In: Glantz MH, Katz RW, Nicholls N (eds) Teleconnections linking worldwide climate anomalies. Cambridge University Press, Cambridge, UK, pp 285–307

Vitousek PM, Mooney HA, Lubchenco J, Melillo JM (1997) Human domination of Earth's ecosystems. Science 277:494–499

Wallace JJ, Gutzler DS (1981) Teleconnections in the geopotential height field during Northern Hemisphere winter. Mon Weather Rev 109:785–812

Wallace JR, Zhang Y, Bajuk L (1996) Interpretation of interdecadal trends in Northern Hemisphere surface air temperature. J Clim 9:249–259

Wiin-Nielson A, Chen T-C (1993) Fundamental of atmospheric energetics. Oxford University Press, New York

Wu Z-X, Newell RE (1998) Influence of sea surface temperature on air temperature in the tropics. Clim Dyn 14:275–290

Xue Y (1997) Biosphere feedback on regional climate in tropical north Africa. Q J R Meteorol Soc 123:1483–1515

Xue Y, Shukla J (1993) The influence of land surface properties on Sahel climate. Part I. Desertification. J Clim 6:2232–2245

Yulaeva E, Wallace JM (1994) The signature of ENSO in global temperature and precipitation fields derived from the Microwave sounding Unit. J Clim 7:1719–1736

Zhang H, Henderson-sellers A, McGuffie K (1997) Impacts of tropical deforestation. Part II: the role of large scale dynamics. J Clim 10:2498–25221

Zhang GJ, McFarlane NA (1995) Sensitivity of climate simulations to the parameterization of cumulus convection in the Canadian Climate Centre general circulation model. Atmos Ocean 33:407–446

Zheng X, Eltahir EAB (1997) The response to deforestation and desertification in a model of West African monsoons. Geophys Res Lett 24:155–158